J. Cosmet. Sci., **61,** 31–38 (January/February 2010)

Modeling the time-dependent water wave stability of human hair

F.-J. WORTMANN, M. STAPELS, and L. CHANDRA,
Textiles & Paper, School of Materials, University of Manchester, PO Box 88, Manchester M60 1QD, UK (F.-J.W.), DWI e. V. and ITMC, RWTH Aachen, Pauwelsstrasse 8, D-52056 Aachen, Germany (M.S.), and Unilever R&D, Port Sunlight, CH63 3JW Wirral, UK (L.C.).

Accepted for publication June 15, 2009. Presented in specific parts at the 3rd International Conference on Applied Hair Science, TRI Princeton, September 15–16, 2008.

Synopsis

The viscoelastic bending recovery of human hair is described by a hydro-rheologically complex, two-phase model, where the humidity dependence of the pertinent parameters as well as the effects of physical aging are known. Model calculations are conducted to assess the consequences of the time- and humidity-dependent bending recovery of human hair for the formation and the stability of the water wave. It is shown that a hair fiber that has been set in bending will achieve at 65% RH a recovery of about 50% after about ten times its storage time prior to release, if it is a non-aging material. However, aging drastically slows the recovery process so that it approaches an apparent "equilibrium," final recovery value of about 60%. The values of final recovery decrease linearly with water content, vanishing as expected at maximum water content, where the hair fiber is above its glass transition. The calculations further show that damage to the elastic modulus, attributed to the intermediate filaments, is expected to reduce recovery and thus enhance fiber set. The calculations demonstrate that it is in fact the phenomenon of physical aging that makes water waving a feasible and practically successful process for hair styling.

INTRODUCTION

In a recent investigations (1) we considered the recovery of human hair from bending deformation in an experimental context related to the formation and stability of a water wave. The bending recovery behavior was determined for a range of humidities and aging times and comprehensively analyzed on the basis of a two-phase filament/matrix model representing the complex morphology of hair. In this model the intermediate filaments (IF) (2), or rather their α-helical fraction, are identified as the filamentous phase in hair. The matrix in consequence contains as major components the amorphous IF-associated proteins (IFAP) (3) and also summarily the rest of the morphological components, such as cuticle, cell membrane complex, etc. (4).

Address all correspondence to F.-J. Wortmann.
The current address of M. Stapels is Kao Chemicals Gmbh, D-46446, Emmerich, Germany.

The matrix of keratins is an amorphous protein that exhibits a strongly humidity-dependent glass transition (5,6). Under most practical conditions, such as 20°C and 65% relative humidity (RH), hair is a semi-crystalline, glassy polymer, for which the viscoelastic properties change continuously due to physical aging (7,8). Furthermore, it was found that both the limiting, short-time elastic modulus of the matrix as well as the speed of the viscoelastic relaxation were affected by water, thus making hair a hydro-rheologically complex (HRC) material (1).

These investigations now explore by model calculations the consequences that derive from the effects of humidity and physical aging on the time-dependent bending recovery of human hair, and which impact on the formation and the stability of the water wave. The results are meant to further contribute to our understanding of the daily consumer practice where bending deformation of hair, set, and recovery under conditions of varying temperature and humidity play an important role for the formation and stability of a hairstyle.

EXPERIMENTAL, THEORETICAL, AND DATA BASIS

The ring test procedure (9,10) was found (1) to be best suited to determine the bending recovery of single hair fibers under various conditions of humidity and physical aging time. Tests, which are the basis of our considerations, were conducted on untreated Caucasian mixed hair. For the test, fibers were wound around 10-mm-diameter glass cylinders and their ends fixed. The cylinders were immersed in distilled water, dried, and subsequently stored for various aging times under controlled humidity conditions at 20°C. After this storage time, the fibers were cut along a line parallel to the cylinder axis, yielding partially opened fiber rings. The recovery of the fiber segments from the rings toward a straight shape was determined by measuring the time-dependent diameters of the rings.

Defining bending set as the retained fraction of initial bending deformation, it is readily shown (9) that the time-dependent set, S, of the fiber at any point around the ring and the diameter, d, of the circle enclosing the partially opened ring are related by:

$$S(t) = d_0 / d(t) \tag{1}$$

where d_0 is the diameter of the cylinder on which the fibers are initially wound and t represents time. Set is related to recovery, R, as the primary parameter to be used in this study:

$$R(t) = 1 - S(t) \tag{2}$$

According to investigations by Chapman (11) and Denby (12), based on the general principles of the viscoelastic properties of polymers (13), the formation and time-dependent recovery of the hairs rings is determined by two antagonistic bending rigidities (stiffnesses) according to:

$$R(t) = B(t)/B(t - \omega) \tag{3}$$

$B(t)$ is the time-dependent bending stiffness at any time after the initial deformation at $t=0$. The fiber is released at $t=\omega$, and $B(t-\omega)$ is accordingly the bending stiffness of the same fiber if it had been bent at the time of release. $B(t)$ relates to the straight fiber and tends to re-straighten it, while $B(t-w)$ derives from the bent state of the same fiber and thus opposes re-deformation. Since both variables act on the same cross-sectional area and shape, R becomes a normalized parameter, for which diameter-related effects are canceled.

Furthermore, it was established (1) that hair shows changes of relaxation behavior with aging time, t_A, which are consistent with Struik's (14) effective time principle and with an aging rate of $\mu=1$ (see equation 10 below). That is, hair bending recovery curves shift on the log-time scale without changing their shape by one decade to higher times with every decade of increase in t_A.

In analogy to the case of extensional relaxation (8,15), time-dependent bending stiffness is described by:

$$B(t) = B_\infty + \Delta B \Psi(t) \tag{4}$$

with

$$\Delta B = B_0 - B_\infty \tag{5}$$

B_0 is the initial value of the bending rigidity at $t=0$. B_∞ is the limiting, elastic stiffness reached by the fiber after complete physical relaxation. Ψ is the relaxation function. In the context of the two-phase model, B_∞ is the contribution of the elastic, partly α-helical filaments, while ΔB is the limiting elastic contribution of the matrix, for which the viscoelastic behavior is described by $\Psi(t)$.

A feasible choice for $\Psi(t)$ is the stretched exponential of the Kohlrausch-Williams-Watts (KWW) function (1,16), given by:

$$\Psi(t) = exp[-(t/\tau)^m] \tag{6}$$

where τ is the characteristic relaxation time and m the shape factor, which give the position and the width of the function on the log-time scale, respectively. It was found (1) that the shape factor of the KWW function was independent of humidity and aging time, with a mean of $m=0.28$, which is close to the universal value of $1/3$ (14).

The relaxation of the matrix contribution to the overall fiber bending stiffness is very fast in water (8,15), where hair is well above its humidity-dependent glass transition (6). This removes all effects of aging and yields effectively $\Delta B=0$ after the wetting of the bent fibers during the initial step of the experiment. A substantial rubber elastic contribution to ΔB, as is expected from the considerations of Hearle *et al.* (17), could experimentally not be verified, namely by Feughelman and Druhala (18), and is thus neglected.

Since this removes the time dependence of the numerator in equation 3, the combination of equations 3 and 4 simplifies to:

$$R(t) = B_\infty / [B_\infty + \Delta B \Psi(t)] \tag{7}$$

for $t_A=const$, where $t=0$ is the start of the recovery experiment. For the analysis of the experimental data, equation 7 is combined with equation 6 and $m=0.28$ to yield:

$$R(t) = 1/\{1 + K\,exp[-(t/\tau)^{0.28}]\} \tag{8}$$

where $K = \Delta B/B_\infty$ is the ratio between the elastic bending rigidities of the filaments and the matrix in the composite, respectively. The initial recovery at $t=0$ is accordingly given by:

$$R_0 = 1/(1 + K) \tag{9}$$

Fitting equation 8 to all experimental curves yielded the values for the rigidity ratio, K, and for the characteristic relaxation time, τ. The mean values for K and the related values for R_0 for the various relative humidities are summarized in Table I. The water content of hair for the various humidities was deduced from sorption isotherms for similar hair material (19).

Consideration of the τ-data versus aging time, t_A, on a log/log-scale (1) showed that $log(\tau)$ shifts synchronously with $log(t_A)$, confirming the value of the expected (14) aging rate, μ, for hair (11) as:

$$\mu = d\log\tau/d\log t_A = 1 \tag{10}$$

To correct for the effects of aging at a given water content, the parameter of the reduced, characteristic relaxation time, τ_r, is introduced:

$$\tau_r = \tau/t_A \tag{11}$$

so that

$$\log\tau_r = \log\tau - \log t_A \tag{12}$$

The results for the arithmetic means of $log\ \tau_r$ are summarized in Table I and discussed in detail in reference 1.

Fibers can be regarded as non-aging as long as the experimental time is small against the aging time, such as $t < 0.1t_A$. For longer times, aging reduces the relaxation rate and induces deviations from the curve expected for the non-aging material (14). For a known aging rate this effect can be compensated by introducing the concept of effective time, λ, given for $\mu=1$ by:

$$\lambda = t_A ln(1 + t/t_A) \tag{13}$$

On the scale of effective time, the experimental data represent the recovery performance of the non-aging fiber. Experimentally, the validity of the concept underlying equations 10–13 has been shown by Chapman, namely, for wool (20).

Table I
Arithmetic Means for $K=\Delta B/B_\infty$ and for the Reduced, Characteristics Relaxation Times, as $log\ \tau_r$

RH (%)	w (%)	K	$log\ \tau_r$	R_0
15	4.0	5.9	0.53	0.14
33	7.8	6.2	0.15	0.14
45	9.5	6.2	0.22	0.14
65	13.0	4.7	0.031	0.18
74	15.1	3.3	−0.13	0.23
82	17.3	2.4	−0.01	0.29

Taken from reference 1.
RH is the relative humidity and w the water content of hair.
R_0 is the value of the initial recovery, given by equation 9.

MODEL CALCULATIONS

To demonstrate the two principal effects of aging on hair fiber recovery, Figure 1 shows the calculated recovery curves at 65% RH for different initial aging times and experimental times well beyond $t=t_A$.

The curves for the hypothetical non-aging hair start close to the time-independent, common value of $R_0=0.18$ at 65% RH (see Table I). The curves follow the path that is prescribed by equation 8 and are shifted on the $log\ \lambda$ scale with respect to the aging time according to equation 10. If the material is non-aging, recovery will be relatively fast and half of the initial set will be lost after about ten times the initial aging time. Deviations between the non-aging and the real, aging material occur at time $t > 1/10t_A$, as marked in Figure 1. Comparison of the curves shows that recovery is drastically slowed through aging. Though small differences are observed with respect to the individual aging time, all recovery curves approach a narrow range of final recovery values around $R_f \approx 0.6$ for very long recovery times ($log\ t > 8$, $t > 3$ years). This is in agreement with practical

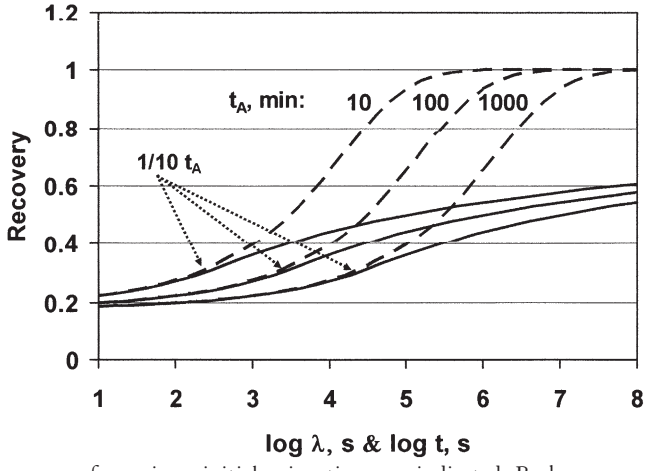

Figure 1. Recovery curves for various, initial aging times, as indicated. Broken curves (---) represent the recovery performance of the hypothetical, non-aging material and relate to the $log\ \lambda$ scale. Solid curves show the behavior of the real, aging material, relating to the $log\ t$ scale. Deviations between the two groups of curves become apparent at $t>1/10\ t_A$, as marked.

observations by the authors as well as with those reported by various informal sources, where water-waved hair tresses have been hanging in laboratories with constant climate for years, apparently without losing their set.

Figure 2 shows the effects of aging on hair recovery curves at different relative humidities and a common, initial aging time (t_A=100 min), calculated on the basis of the parameter values given in Table I for non-aging and for aging hair, respectively. Again, aging greatly delays recovery, and the recovery values, which the curves apparently approach for long times, increase with increasing relative humidity. This is in agreement with the practical observation that the set of a hairstyle based on water waving decreases with increasing humidity.

Figures 1 and 2 show that for long times recovery approaches an apparent constant value. In order to calculate the "equilibrium," the apparent final value of recovery, R_f, for the different humidity conditions, and for all practical purposes a very long time ($log\ t$=11, t>3000 years), was chosen. The values for R_f are summarized in Figure 3 versus water content. The values closely follow a straight line, which describes the loss of set with increasing humidity. The straight line fit predicts R_f =0.32 for dry hair and total recovery at a water content of about 25%. The latter value is in good agreement with the maximum water content of hair. The extrapolation validates the assumption underlying the calculations that total recovery will be achieved in water, that is, at conditions above the glass transition. Furthermore, the observation is in good agreement with the practical observation that wetting of hair removes the water wave.

The tools that have been developed for the above calculations also enable as to assess the effects of fiber damage on bending recovery; namely, DSC-investigations (21,22) have shown that, damage, e.g., through oxidative or reductive processing, is first and most strongly imparted to the filaments. Plausibly expecting that such damage will lower the elastic modulus of the filaments, Figure 4 shows recovery curves for an undamaged hair at 65% RH and a constant, short aging time of t_A=10 min, together with the recovery

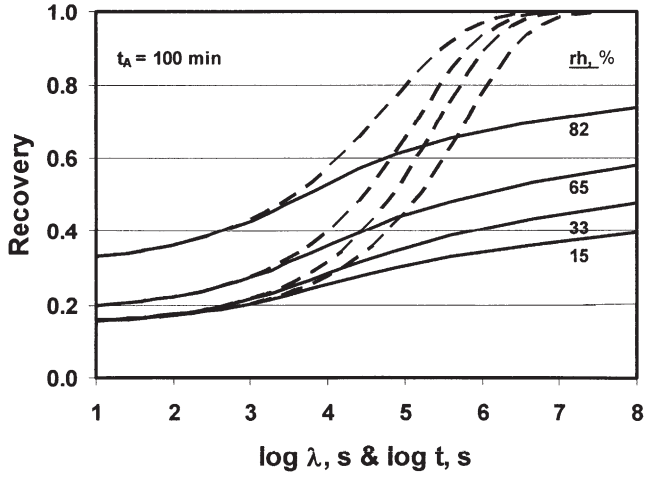

Figure 2. Recovery curves at constant aging time (t_A=100 min) and for different relative humidities (20°C), as marked for the solid curves for the aging material. The broken lines show the related curves, expected for non-aging hair.

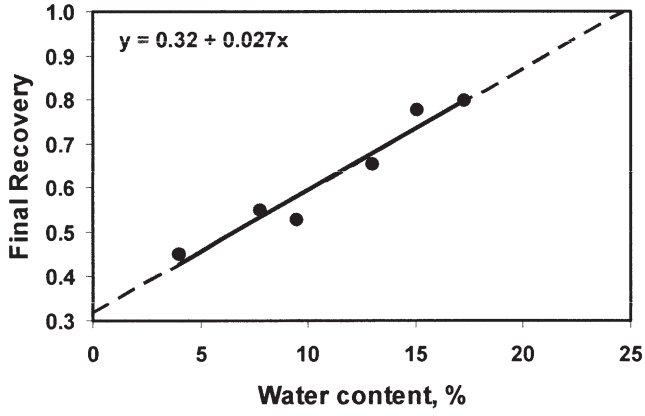

Figure 3. Recovery values of aging hair at *log t = 11* (*t* > 3000 years), considered as representing "equilibrium," final recovery, R_f, for all practical purpose, vs water content. A straight line is fitted through the data, for which the equation is given on the graph in the usual x/y-notation. The broken line marks the extrapolation range.

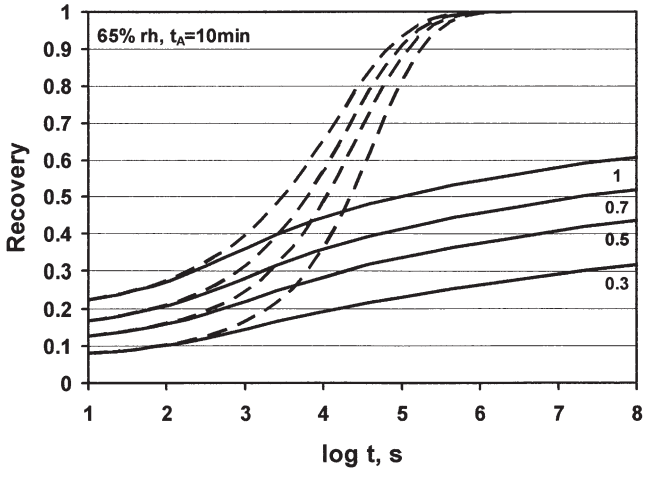

Figure 4. Bending recovery curves of non-aging (broken lines) and aging hair (solid lines) at 65% RH and t_A*=10 min,* in which the elastic bending stiffness of the filaments, B_∞, has been reduced from the initial, relative value of 1 to 0.7, 0.5, and 0.3, respectively. The curves for the aging material are marked accordingly.

of the same material in which the bending stiffness of the filaments, B_∞, is reduced to relative values of 70%, 50%, and 30%, respectively, while that of the matrix ΔB is kept unchanged. Figure 4 shows that damage to the elastic fraction of fiber bending stiffness is expected to significantly promote and stabilize the set for the aging fiber, while the effect in the non-aging fiber will eventually be lost. In practice, however, the beneficial effects of filament damage are expected to be offset through collateral processing damage to the matrix and other morphological components, as well as the expected higher susceptibility of damaged hair to humidity and temperature changes, which will remove the benefits of physical aging.

CONCLUSIONS

The model calculations show, in agreement with practical observations, that the relative humidity of the environment as well as hair damage have an important influence on the performance of a non-permanent hairstyle on the basis of water waving. However, irrespective of the environmental conditions, as long as they stay below the glass transition, it is nevertheless the phenomenon of physical aging that makes water waving a feasible and practically successful process for hair styling.

REFERENCES

(1) F.-J. Wortmann, M. Stapels, and L. Chandra, Humidity dependent bending recovery and relaxation of human hair, *J. Appl. Polym. Sci.,* **113**, 3336–3344 (2009).
(2) M. Feughelman, *Mechanical Properties and Structure of Alpha-Keratin Fibers* (University of New South Wales Press, Sydney, Australia, 1997).
(3) D.A.D. Parry and P. Steinert, Intermediate filaments: Molecular architecture, assembly, dynamics and polymorphism, *Quarterly Rev. Biophys.,* **32,** 99–187 (1999).
(4) H. Zahn, F.J. Wortmann, G. Wortmann, K. Schaefer, R. Hoffmann, and R. Finch, "Wool," in *Ullmann's Encyclopedia of Industrial Chemistry,* 6th ed. (Wiley-VCH, Weinheim, Germany, 2003), Vol.39.
(5) F.J. Wortmann, B.J. Rigby, and D.G. Phillips, Glass transition temperature of wool as a function of regain, *Text. Res. J.,* **54,** 6–8 (1984).
(6) F.J. Wortmann, M. Stapels, R. Elliott, and L. Chandra, The effect of water on the glass transition of human hair, *Biopolymers,* **81,** 371–375 (2006).
(7) B.M. Chapman, The aging of wool. Part I: Aging at various temperatures, *J. Text. Inst.,* **66,** 339–342 (1975).
(8) F.J. Wortmann and S. DeJong, Analysis of the humidity-time superposition for wool fibers, *Text. Res. J.,* **55,** 750–756 (1985).
(9) F.-J. Wortmann and I. Souren, Extensional properties of human hair and permwaving performance, *J. Soc. Cosmet. Chem.,* **38,** 125–140 (1987).
(10) F.-J. Wortmann and N. Kure, Bending relaxation properties of human hair and permwaving performance, *J. Soc. Cosmet. Chem.,* **41,** 123–139 (1990).
(11) B.M. Chapman, The rheological behaviour of keratin during the aging process, *Rheol. Acta,* **14,** 466–470 (1975).
(12) E.F. Denby, A note on the interconversion of creep, relaxation and recovery, *Rheol. Acta,* **14,** 591–593 (1975).
(13) J.D. Ferry, *Viscoelastic Properties of Polymers* (John Wiley & Sons; New York, 1980).
(14) L.C.E. Struik, *Physical Aging in Amorphous Polymers and Other Materials* (Elsevier, Amsterdam, 1978), Chapter 4.
(15) F.J. Wortmann, The viscoelastic properties of wool and the influence of some specific plasticizers, *Colloid Polym. Sci.,* **265,** 126–133 (1987).
(16) C.A. Angell, K.L. Ngai, G.B. McKenna, P.F. McMillan, and S.W. Martin, Relaxation in glassforming liquids and amorphous solids, *J Appl. Phys.,* **88,** 3113–3157 (2000).
(17) J.W.S. Hearle, B.M. Chapman, and G.S. Senior, The interpretation of the mechanical properties of wool, *Appl. Polym. Symp.,* **18,** 775–794 (1971).
(18) M. Feughelman and M. Druhala, The lateral mechanical properties of alpha-keratin, *Proc. 5th Int. Wool Text. Res. Conf. Aachen,* **II,** 340–349 (1976).
(19) F.J. Wortmann, A. Hullmann, and C. Popescu, Water management of human hair, *IFSCC Mag.,* **10,** 317–320 (2007).
(20) B.M. Chapman, Linear superposition of time-variant viscoelastic responses, *J. Phys. D: Appl. Phys.,* **7,** L185–L188 (1974).
(21) F.-J. Wortmann, C. Popescu, and G. Sendelbach, Nonisothermal denaturation kinetics of human hair and the effects of oxidation, *Biopolymers,* **83,** 630–635 (2006).
(22) F.J. Wortmann, C. Popescu, and G. Sendelbach, Effects of reduction on the denaturation kinetics of human hair, *Biopolymers,* **89,** 600–605 (2008).